Evaluation of the Serotonin Transporter Ligand ^{123}I-ADAM for SPECT Studies on Humans

Vibe G. Frokjaer[1], Lars H. Pinborg[1], Jacob Madsen[2], Robin de Nijs[1,3], Claus Svarer[1], Aase Wagner[4], and Gitte M. Knudsen[1]

[1]Neurobiology Research Unit, Copenhagen University Hospital Rigshospitalet, Copenhagen, Denmark; [2]PET and Cyclotron Unit, Copenhagen University Hospital Rigshospitalet, Copenhagen, Denmark; [3]Danish Magnetic Resonance Center, Hvidovre University Hospital, Hvidovre, Denmark; and [4]Diagnostic Radiology, Copenhagen University Hospital Rigshospitalet, Copenhagen, Denmark

Imaging serotonin transporters in the living human brain is important in several fields, such as normal psychophysiology, mood disorders, eating disorders, and neurodegenerative disorders. The aim of this study was to compare different kinetic and semiquantitative methods for assessing serotonin transporters using ^{123}I-labeled 2-((2-((dimethylamino)methyl)phenyl)thio)-5-iodophenylamine (ADAM) in humans: an arterial plasma input model, simplified and Logan reference tissue models, and standardized uptake value ratios. **Methods:** Nine subjects were scanned with dynamic ^{123}I-ADAM SPECT (mean age, 31 y; range, 24–43 y), and metabolite-corrected arterial input was measured. Tissue reference models (simplified reference tissue model, Logan reference tissue model, and ratio method) were validated against the outcome of a 1-tissue-compartment model, and performance with decreasing scan length was evaluated. The specificity of ^{123}I-ADAM binding was investigated in a blocking experiment. **Results:** Binding estimates from the simplified reference tissue and Logan reference tissue models correlated tightly with full kinetic modeling when based on a 240- or 360-min dynamic acquisition ($r = 0.99$); however, there were slight underestimations (3%–5%), especially in high-binding regions. Application of the ratio method to data from 200 to 240 min overestimated specific binding (on average, by 10% ± 28%) and correlated only moderately with estimates from the 1-tissue-compartment model ($r = 0.94$). With an acquisition time of 0–120 min, the Logan model still yielded an acceptable outcome when a fixed clearance rate constant (k2′) from the cerebellum was applied. Intravenously injected citalopram was not associated with a decrease in cerebellar binding. A lipophilic metabolite that did not seem to bind specifically to serotonin transporter was seen in 2 of 7 subjects. **Conclusion:** Serotonin transporter binding with ^{123}I-ADAM SPECT can be assessed with the Logan model based on a 120-min acquisition when a constant k2′ is applied. This model, because it allows for more accurate and less biased binding estimates and thus reduces the required sample size, is advantageous over the ratio method used in clinical studies so far. A single blocking experiment supported the use of the cerebellum as a reference region.

Key Words: neurology; SPECT; radiotracer tissue kinetics; brain imaging; serotonin transporter

J Nucl Med 2008; 49:247–254
DOI: 10.2967/jnumed.107.046102

The serotonergic system is involved in normal psychophysiology and in the pathophysiology of several neuropsychiatric disorders, such as neurodegenerative disorders, obsessive compulsive disorder, Tourette's syndrome, and mood and eating disorders (*1,2*). Serotonin transporter is located presynaptically on the cell bodies and terminals of serotonergic neurons and is a marker of serotonergic innervation (*3*). The serotonin transporter binding site clears serotonin from the serotonergic synapse and also enables recycling of the neurotransmitter. Several antidepressants act on the serotonin transporter binding site. Therefore, imaging of serotonin transporter is of great scientific, and potentially clinical, value in studies of normal psychophysiology, in studies of the pathophysiology of neuropsychiatric disorders, and in evaluations of the mechanisms of action and monitoring of antidepressive treatment.

^{11}C-labeled 2-((2-((dimethylamino)methyl)phenyl)thio)-5-iodophenylamine (ADAM) has proven useful as a PET tracer for in vivo serotonin transporter imaging, but in baboons, ^{11}C-DASB has proven superior to ^{11}C-ADAM because of faster kinetics and a higher signal-to-noise ratio (*4*). The SPECT counterpart of ^{11}C-ADAM, ^{123}I-ADAM, has so far been the ligand of choice for SPECT imaging of serotonin transporter. The primary advantages of SPECT over PET are the lower costs and the easier-to-handle longer-lived radioligands. ADAM displays a high affinity for serotonin transporter binding sites (inhibition constant [K_i], 0.013 nM) and is 10,000-fold more selective for serotonin transporter than are the specific monoamine dopamine transporter (K_i, 840 nM) and the specific monoamine norepinephrine transporter (K_i, 699 nM), as measured by a competition binding assay based on 3 LLC-PK_1 cell lines from pig kidney expressing the 3 transporters (*5*). The effective dose of

Received Aug. 7, 2007; revision accepted Sep. 21, 2007.
For correspondence or reprints contact: Vibe G. Frokjaer, MD, Neurobiology Research Unit 9201, Copenhagen University Hospital, Rigshospitalet, Blegdamsvej 9, DK-2100 Copenhagen, Denmark.
E-mail: vibe@nru.dk

radiation when imaging with ^{123}I-ADAM is 0.036 mSv/MBq (*6*).

Twelve clinical studies involving more than 200 subjects have already been conducted with ^{123}I-ADAM SPECT (*7–18*) (supplemental Table 1 [supplemental materials are available online only at http://jnm.snmjournals.org]), but so far the quantification has been based on a ratio method that relates the standardized uptake value in a target region to that in a reference tissue region, and so far, no study on humans has evaluated the ratio method against full kinetic modeling with arterial plasma input. Also, the ^{123}I-ADAM metabolites and the in vivo selectivity of the ligand need to be assessed in humans.

In this study, we evaluated the simplified reference tissue model (*19*), the Logan reference tissue model (*20*), and the ratio method, using input from the cerebellum as the reference region, against full kinetic modeling with arterial input. The performance of the reference tissue models with reduced acquisition times was also evaluated. Further, we assessed ^{123}I-ADAM metabolites and studied the specificity of ^{123}I-ADAM binding through a blocking experiment with injection of a selective serotonin reuptake inhibitor (SSRI) during image acquisition.

MATERIALS AND METHODS

Subjects

Nine healthy volunteers, 6 men and 3 women, with a mean age of 31 y (range, 24–43 y) participated in the study. In 2 subjects, arterial input was not available. Thus, full kinetic modeling could be done in 7 subjects, whereas data from all 9 subjects were available for simplified reference tissue modeling. In 2 subjects, a blocking study with intravenous infusion of citalopram during acquisition was done. The study was approved by the local Ethic Committee under protocol KF 02-150/98 (amendment KF 12-084/02). All subjects gave written informed consent to participate in the study.

SPECT Imaging and Acquisition

After injection of 3.2 ± 0.78 MBq (mean ± SD) of ^{123}I-ADAM per kilogram of body weight, dynamic SPECT was conducted over a period of 5.5 or 6 h beginning immediately on injection. The protocol consisted of 30 frames of 2 min each, followed by between 27 and 30 frames of 10 min each. Five subjects underwent a blocking experiment with citalopram during the dynamic acquisition. In these cases, the scanning sequence was modified to include 45 scans of 2 min each, obtained between 4 and 5.5 h. However, only 2 subjects tolerated the full blocking paradigm. To minimize movement during the scan, we used a headband to lightly fix the head of each subject. To block thyroidal uptake of free radioiodine, we gave each subject 200 mg of potassium perchloride intravenously 30 min before injection of ^{123}I-ADAM. SPECT was performed on a triple-head IRIX camera (Philips) fitted with low-energy, general-purpose parallel-hole collimators. The system resolution (full width at half maximum) was approximately 8.4 mm at 10 cm (IRIX product data sheet). The mean radius of rotation was 14.4 cm (range, 13.6–14.5 cm). To allow later correction for septal penetration and backscatter from high-energy photons, we recorded the signal in 2 separate energy windows. Window 1 was centered at 159 keV, with a width of 32 keV, and window 2 was centered at 200 keV, with a width of 32 keV. Each camera head covered 120° of the circular orbit. Scanning was performed in continuous mode, and projection data were acquired with 40 angular steps of 3° each. The acquisition matrix was 128 × 128, with a pixel size of 2.33 mm in both directions.

Reconstruction

The projection image files were exported in Digital Imaging and Communications in Medicine format using the scanner software (Odyssey 9.2B; Philips). The exported files were transferred to a UNIX platform for further processing by routines developed at the Neurobiology Research Unit. Before reconstruction of the projection images, the raw data of the 2 energy windows were subtracted in sinogram space to correct for penetration and backscatter from high-energy photons. The number of counts in the high-energy window was multiplied by 1.1, the factor being determined by recording the 2 energy windows of a ^{123}I-source contained in 6-mm-thick lead. Reconstruction was performed using standard filtered backprojection with a spheric 3-dimensional low-pass fourth-order Butterworth postprocessing filter with a cutoff frequency of 0.3 Nyquist (0.064 mm^{-1}) and using uniform attenuation correction with an attenuation coefficient of 0.11. The complete subtraction and reconstruction algorithm was performed in Matlab 6.5 (The MathWorks, Inc.). The resulting series of images was written as a dynamic Analyze file.

All frames from 2 to 6 h were aligned using the automated image registration algorithm, version 5.2.5 (*21*). The 2-min frames acquired for the first hour did not contain enough information to be aligned. Before alignment, each frame was filtered with a 12-mm gaussian filter, and a threshold was applied at the 85% fractile of the voxel counts in the image. These parameters were chosen by visual inspection of threshold-constrained images to ensure that they included brain gray matter voxels. The rigid transformation was estimated for each frame to a selected single frame with sufficient structural information (60–70 min after injection) using the scaled least-squares cost function in the automated image registration algorithm. Subsequently, frames were resliced and converted to a dynamic Analyze image file format.

Structural Imaging

All subjects underwent a structural MRI scan on a 1.5-T Vision scanner (Siemens) using the 3-dimensional magnetization-prepared rapid gradient-echo sequence (inversion time/delay time/echo time/repetition time, 300/300/4.4/11.4 ms; flip angle, 12°) acquired as sagittal plane scans with a spatial resolution of 1.50 × 1.13 × 1.02 mm. There were 130 planes, and the in-plane matrix was 230 × 256.

Coregistration, Delineation of Volumes of Interest, and Partial-Volume Correction

SPECT and MR images were coregistered using a Matlab-based program in which SPECT and MR images were brought into alignment through manual translation and rotation of the SPECT image with subsequent visual inspection in 3 planes. Seven volumes of interest (thalamus, midbrain, caudatus, putamen, occipital cortex, superior frontal cortex, and cerebellum) were automatically delineated on the MR images and directly transferred to the coregistered SPECT image, by a method based on probability mapping, as described in detail by Svarer et al. (*22*). To enable partial-volume correction of the SPECT data, we segmented the MR images into gray matter, white matter, and cerebrospinal fluid tissue using statistical parametric mapping (SPM2; Wellcome Department of

Cognitive Neurology). Partial-volume correction was performed according to the method of Muller-Gartner (*23*). The white matter value was extracted as the mean voxel value from a predominantly white matter volume of interest (midbrain) in the uncorrected SPECT image (*24*).

Time–activity curves were extracted from the 7 volumes of interest as a volume-weighted average of left and right regions and subsequently used for modeling. In the simplified quantification model, the cerebellum was used as a reference region, representing nonspecific binding only because the cerebellar vermis is not included in the cerebellar volume of interest (*22,25*).

Input Function Measurement

Arterial blood samples were collected from 7 subjects every 10 s for the first 2 min and at 3, 5, 10, 15, 20, 30, 40, 50, 65, 85, 105, 135, 165, 195, 225, 255, 285, 315, 345, and 360 min after injection. Samples were kept on ice when transported for analysis. After centrifugation, 500 μL of plasma were collected and the activity was measured with a γ-counter (Cobra 5003; Packard Instruments). Fractions of parent compound and labeled metabolites were determined by high-performance liquid chromatography (HPLC) after solid-phase extraction on samples collected beginning at 3 min after injection. With solid-phase extraction, plasma supernatant (5 mL) was added to an aqueous solution of acetic acid (20 mL, 50 mM) and eluted through a C18 Sep-Pak cartridge (Waters). The Sep-Pak column was then washed with an aqueous triethylamine solution (10 mL, 0.1%) followed by deionized water (10 mL) and eluted with methanol (2 mL). The eluent was filtered with an HV syringe filter (Millipore), and an equal volume of deionized water was added to the filtrate. Four milliliters of this sample were injected in the HPLC column. Five micrograms of cold ADAM were added as a carrier and to allow identification of the retention time of ^{123}I-ADAM in the ultraviolet spectrum. For HPLC, the column was a μBondapak C-18 (7.8 × 300 mm, 10 μm; Waters) and the eluent was 0.01 M phosphoric acid (solvent A) and acetonitrile (solvent B). The solvents were mixed 75/25 and gradually increased to 40/60 over 10 min, at a flow rate of 3 mL/min. The retention time for the parent compound varied from 10 to 12 min between subjects. To enable comparison of activity measurements between the SPECT scanner and the γ-counter, cross calibration with a phantom containing a known concentration of ^{123}I-labeled tracer was performed.

To evaluate the stability of ^{123}I-ADAM in blood, we took 3 blood samples from each of 7 subjects. One sample was analyzed by HPLC immediately; one, after being kept on ice for 30 min; and one, after being kept at room temperature for 1 h.

Blocking

Starting 4 h from injection, 5 subjects received intravenous infusions, over 30 min, of citalopram (0.25 mg/kg) to block specific serotonin transporter binding. Because of unacceptable side effects, 3 subjects received only a reduced dosage (0.05, 0.07, and 0.11 mg/kg) The side effects, which included nausea, a sensation of heat, a drop in blood pressure, and in 1 person vomiting, were reversed within a few minutes, allowing continuation of the acquisition except for a short break in 1 case. Thus, 2 subjects completed the full intravenous blocking paradigm.

Kinetic Analysis

Serotonin transporter binding was quantified by kinetic analysis of the regional time–activity curves and arterial input curves with the 1-tissue-compartment (1TC) model, the 2-tissue-compartment model, and the reference tissue models (simplified and Logan) by use of PMOD software, version 2.85 (PMOD Technologies). The ratio method was derived as (total binding/nonspecific binding − 1), based on the regional mean counts in the intervals from 220 to 240 min and from 200 to 240 min after injection. For the Logan model, 2 versions were applied. The first of these used an individual estimate of the clearance rate constant from the cerebellum (k2′). k2′ was fitted individually by applying simplified reference tissue model 2 (PMOD 2.85) on volume-weighted mean time–activity curves from high-binding regions (caudate, thalamus, and putamen). This k2′ estimate was entered in the Logan model (Logan noninvasive, PMOD 2.85) (*20*). The mean estimated k2′ (±SD) was 0.032 ± 0.010. The second Logan model was one in which k2′ was neglected by entering the cerebellar time–activity curves as arterial input (Logan invasive, PMOD 2.85). The resulting binding estimate then corresponded to $BP_{ND} + 1$. Linear start times were not fixed in either model.

Further, the performance of the reference tissue models (simplified and Logan with k2′) at shorter acquisition times (240, 180, 120, 90, and 60 min) was tested. Nine subjects entered this part of the analysis. Two versions of the Logan model with k2′ were explored, one with a constant k2′ (mean k2′ for the longest time–activity curves) and another with k2′ modeled to each individual time–activity curve. Linear start times were not fixed.

Comparison of Reference Tissue Models Against Full Kinetic Models Using Arterial Input

Use of the 2-tissue-compartment model was associated with an unacceptable number of nonconvergence or large errors in estimates of regional total distribution volume (V_T). In 3 of 7 subjects, the 2-tissue-compartment model did not apply. Therefore, the 1TC model was selected as the more appropriate gold-standard full kinetic model. Similar observations about the better fit of 1TC models have been reported for other serotonin transporter tracers (*26*). To compare the binding potential derived from the 1TC model ($BP_P = V_T - V_{ND}$) with the binding potentials derived from the reference tissue models (BP_{ND}), we calculated the distribution volume of specific binding ($V_T - V_{ND}$) divided by the distribution volume in the reference region (V_{ND}) on the basis of the outcome parameters from the 1TC model. The parameters are related as follows: $BP_{ND} = BP_P/V_{ND} = (V_T - V_{ND})/V_{ND} = V_T/V_{ND} - 1$ (*27*). The estimated BP_{ND} from the 1TC model and the BP_{ND} from the simplified model were compared by linear regression and 2-tailed paired *t* tests. Also, the pairwise percentage difference between BP_{ND} values, as compared with the 1TC estimate, was calculated and reported as mean difference in percentage ± SD.

RESULTS

Average time–activity curves for regional uptake of ^{123}I-ADAM are displayed in Figure 1, and an example of the ^{123}I-ADAM binding distribution in the human brain is illustrated in Figure 2. Table 1 shows the outcome of the different models: The highest BP_{ND} values were found in the thalamus, followed by the putamen, midbrain, caudate, frontal cortex, and occipital cortex.

Comparison of Reference Tissue Models Against Full Kinetic Modeling Using Arterial Input

Correlations between the 1TC and reference tissue models are illustrated in Figure 3. For 2 subjects, the simplified reference tissue model grossly overestimated midbrain BP_{ND};

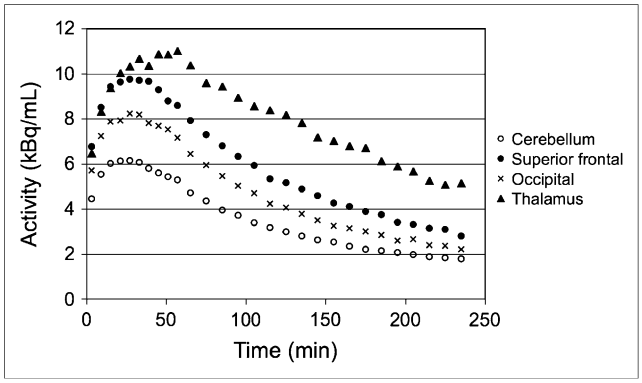

FIGURE 1. Time–activity curves for regional uptake of ^{123}I-ADAM generated as average of data from 7 subjects. In low-density regions (cerebellum and occipital cortex), uptake peaked at around 20–30 min. High-density regions (thalamus displayed) peaked later, at around 40–50 min.

hence, the correlation with the 1TC model was moderate (r = 0.949). Leaving out the 2 outliers yielded a tight correlation (r = 0.994), but the simplified reference tissue model significantly underestimated BP_{ND} by 3% ± 7% (P = 0.03).

The outcomes of both Logan reference tissue models correlated tightly with the 1TC model (Logan with k2′, r = 0.992; Logan without k2′, r = 0.994). Both models significantly underestimated BP_{ND}, on average by 5% (Logan with k2′, 5% ± 8%, P = 0.0003; Logan without k2′, 5% ± 5%, P = 0.000002). However, Logan without k2′ underestimated high-binding regions more than Logan with k2′ did (linear equations: Logan with k2′, y = 0.97x − 0.005; Logan without k2′, 0.94x + 0.016) (Supplemental Fig. 1).

The ratio method with time–activity curves for 200–240 min by contrast significantly overestimated BP_{ND}, compared with the 1TC model, on average by 10% ± 28% (P = 0.00007; Fig. 3C). The overestimation was more pronounced in high-binding regions (linear equation: y = 1.256x − 0.0965). Also, the correlation between the ratio

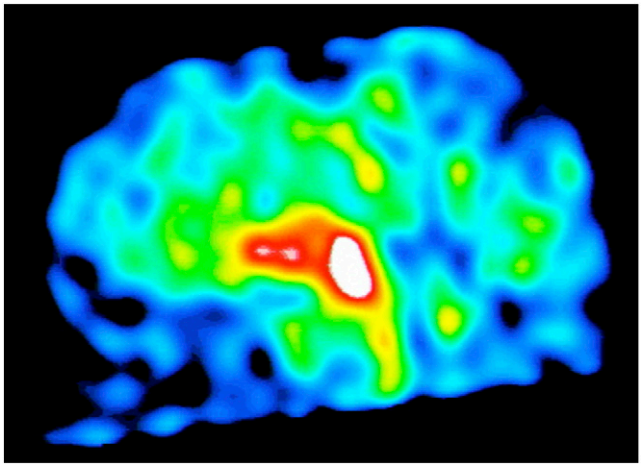

FIGURE 2. ^{123}I-ADAM binding in healthy 39-y-old man. View is sagittal, with nose left; slice is 4.67 mm. Image is based on data from 180 to 240 min after injection.

method and the 1TC model was moderate at 200–240 min after injection (r = 0.94) and worse at 220–240 min after injection (r = 0.92). For the 3 subjects who did not receive blocking, the ratio derived from 240 to 280 min (y = 1.29x − 0.115, r = 0.946) was as biased as, and correlated less tightly than, the ratio from 200 to 240 min (y = 1.32x − 0.142, r = 0.968) (Supplemental Fig. 2).

Effect of Reducing Acquisition Times for the Reference Tissue Models

The simplified reference tissue model failed to converge in at least 1 region in the following instances: in 3 cases when the time–activity curve was reduced to 180 min, in 2 cases when it was reduced to 120 min, in 1 case when it was reduced to 90 min, and in 3 cases when it was reduced to 60 min. The Logan reference tissue model with k2′ was more stable and did not fail to converge in any instance. Figure 4 shows the average normalized binding for time–activity curves at different intervals. The model yielded acceptable values for time–activity curves of 120-min duration, compared with time–activity curves for 0–240 min. For the thalamus, BP_{ND} values estimated using 90-min time–activity curves differed significantly from BP_{ND} values estimated using an acquisition of 0–240 min. The values were underestimated by 17% ± 14% (P = 0.005) on average. For the superior frontal region, only the binding estimate based on 0–180 min was significantly overestimated, by 2% ± 2%, but it correlated tightly with the value based on 0–240 min (P = 0.02) and was practically unbiased (r = 0.999, y = 1.003x + 0.010) compared with that value. For the occipital cortex, the values from 180 min (P = 0.01) and 120 min (P = 0.0004) were slightly but significantly overestimated yet correlated tightly (4% ± 2%, r = 0.999, and 8% ± 9%, r = 0.991, respectively) with the value from 240 min (Supplemental Fig. 3).

Metabolites

The time course of fractional unchanged ^{123}I-ADAM varied from subject to subject and typically was around 50% at 20 min, decreasing to 5%–12% at 3–4 h after injection. A labeled lipophilic metabolite was detected in 2 of 7 subjects (retention time, 17.7 min), as illustrated in Figure 5. The fraction of this lipophilic metabolite peaked at approximately 90–120 min after injection, when it constituted about 13%, and remained fairly constant throughout the experiment. The concentration of parent compound increased after blocking with citalopram (0.25 mg/kg) whereas the concentration of the lipophilic metabolite remained constant, suggesting that this metabolite does not bind specifically to serotonin transporters in platelets or lung tissue. Labeled hydrophilic metabolites, most often 2, were detected in all subjects.

Stability of ^{123}I-ADAM

Unlike the samples analyzed immediately, ^{123}I-ADAM and its metabolites when placed on ice remained unchanged for 30 min in whole blood. When kept at room temperature for 60 min before analysis, 1% of the ^{123}I-ADAM was lost,

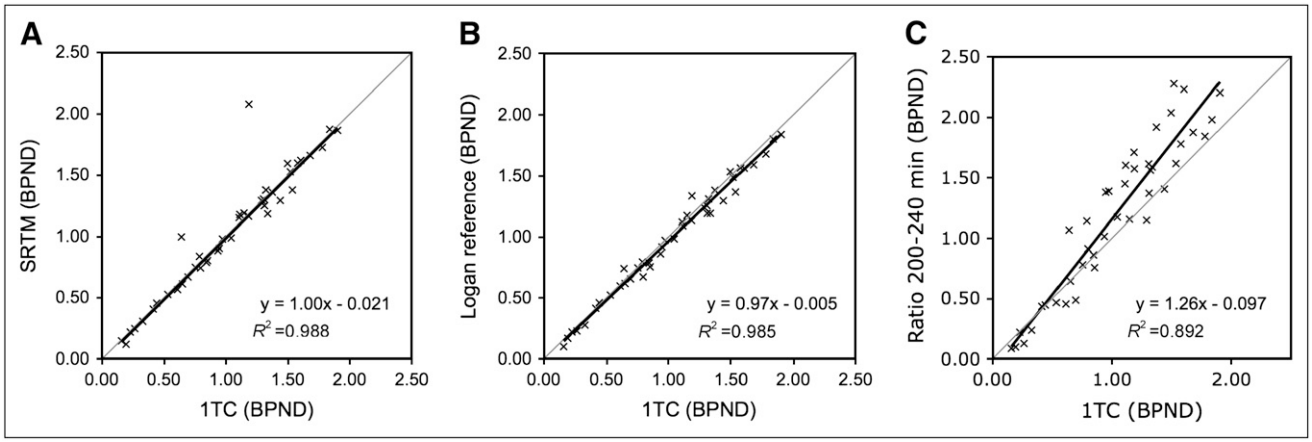

FIGURE 3. Comparison of 1TC and reference tissue methods. (A) Compared with 1TC, the simplified reference tissue model grossly overestimated midbrain BP_{ND} for 2 subjects, resulting in a modest correlation (r = 0.949). When the 2 outliers were excluded, simplified reference tissue model correlated tightly with 1TC model (r = 0.994) and only slightly underestimated BP_{ND} (3% ± 7%, P = 0.03). (B) BP_{ND} estimates from 1TC and Logan reference models (Logan ref_1, where k2′ is estimated individually from simplified reference tissue model) correlated tightly (r = 0.992). Logan reference model slightly underestimated BPND, more so in high-binding regions (5% ± 8%, P = 0.0003). (C) Correlation between 1TC and ratio method was acceptable both when based on 40-min acquisition (r = 0.94) and when based on 20-min acquisition (linear equation: y = 1.188x − 0.065, R^2 = 0.8421, r = 0.92). However, ratio method substantially overestimated BP_{ND}, on average by 10% ± 28% (P = 0.00007), and overestimation was most pronounced in high-binding regions.

probably because of a minor degree of metabolism, as described in an earlier publication (*28*).

Blocking

Time–activity curves of brain uptake of tracer before and after SSRI blocking were associated with tracer displacement in high-density regions but not in the cerebellum. This finding indicates that cerebellar binding represents nonspecific binding only (Fig. 6).

DISCUSSION

To our knowledge, this was the first study on humans to validate reference tissue methods of quantification of serotonin transporter with ^{123}I-ADAM SPECT against a gold standard, namely a full kinetic model with arterial input. We found that the Logan reference tissue model based on a 240-min acquisition, with or without inclusion of k2′, correlated tightly with full kinetic modeling and only slightly underestimated specific binding, by around 5%, mostly in high-binding regions. It is a well-described phenomenon that the Logan model underestimates receptor binding in the presence of noise, especially in high-binding regions (*29*). Our data indicate that the bias is smaller with the Logan reference model using a k2′ estimate from a large subcortical region. The simplified reference tissue model underestimated BP_{ND} less than did the Logan reference model—around 3%—but in 2 of 7 subjects had difficulty in quantifying the midbrain. This finding confirms a previous study on baboons that also found the simplified reference tissue model to underestimate specific binding, with an increasing bias for high-density regions (*30*). The clinical studies published so far have recommended use of a ratio between specific binding regions and cerebellum that includes time–activity curves from 200 to 360 min after injection, with a total acquisition time of 30–60 min (*7,9,10,17*). This recommendation is based on comparisons with simplified reference tissue model estimates from data generated by sequential acquisitions at 5.5–7 h after injection. We found that the ratio method, when based on time–activity curves from 200–240 min or 240–280 min after injection, significantly overestimated specific binding in humans, and more so in high-binding regions—by 10% ± 28% on average. This bias is consistent with theoretic predictions that the ratio of specific tissue uptake to nonspecific tissue uptake during transient equilibrium overestimates the ratio at true equilibrium, because of the more rapid clearance from plasma than from tissue (*31*). The

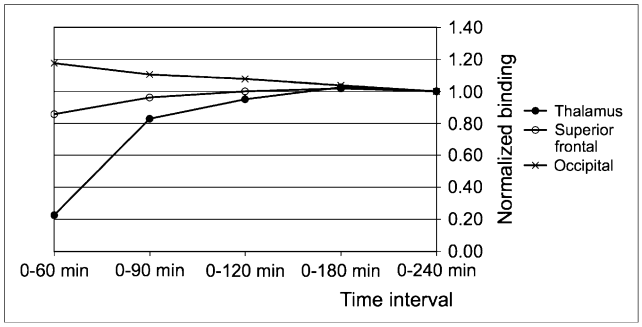

FIGURE 4. Average normalized specific binding in thalamus, occipital cortex, and superior frontal cortex calculated from Logan reference model (with cerebellum as reference and k2′ fixed to 0.0311) at reduced acquisition intervals. Normalization was performed by dividing BP_{ND} value calculated using each time interval by value obtained on basis of time–activity curves from 0 to 240 min. Logan reference model yielded acceptable values for time–activity curves of 120-min duration, compared with time–activity curves based on 0–240 min.

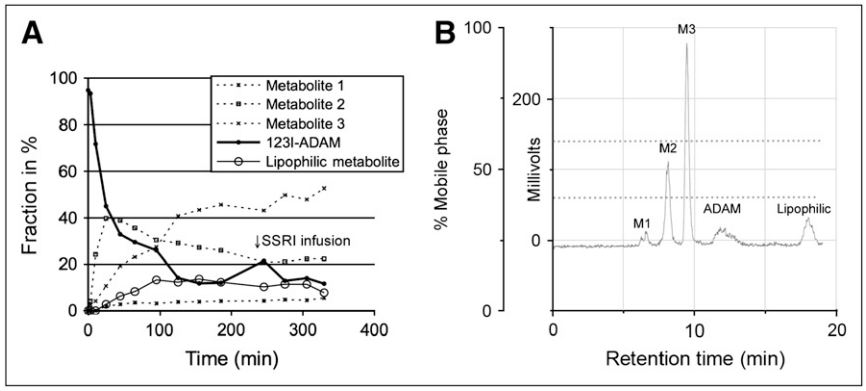

FIGURE 5. (A) Fraction of parent compound and labeled metabolites of ^{123}I-ADAM over time, from subject with lipophilic metabolite. Fraction of parent compound increased after blocking at 240–270 min, whereas fraction of lipophilic metabolite did not. (B) Output from HPLC analysis of sample from 195 min after injection with lipophilic metabolite.

largest errors are seen in high-binding regions. The time point of transient equilibrium depends on the region assessed: The higher the binding, the later the time. The extent of the overestimation also depends on the plasma clearance rate, which will vary from subject to subject and, unfortunately, in some instances, even more so between patients and healthy controls. Accordingly, ^{123}I-ADAM studies on humans have shown the ratio method to have a poor test–retest outcome, with intrasubject variability of 13% ± 11% in the midbrain, 16% ± 13% in the thalamus, and around 20% in the lower-binding regions (*7*). Thus, larger sample sizes are required with this approach. With the sample sizes of 10–44 subjects used in previous ^{123}I-ADAM imaging studies, only major differences would be detectable. Accordingly, occupancy calculations based on the ratio method have been highly variable (*17*).

As an alternative to the ratio method, we explored the performance of the simplified reference tissue model and the Logan reference tissue model with k2′ and reduced acquisition times. The simplified model failed to apply in 3 subjects and was found not to be operational at reduced scan times. The Logan model was more stable: BP_{ND} based on time–activity curves that included only the first 120 min was still reliably quantified in regions of high (thalamus), intermediate (superior frontal), and low (occipital) binding. However, binding in the occipital cortex correlated tightly with the values for 0–240 min yet was slightly overestimated, compared with those values (8% ± 9%, r = 0.991, P = 0.0004 [paired t test, uncorrected]).

In the clinical setting, the importance of a tolerable acquisition protocol is paramount. Therefore, if the acquisition time is to be kept low, ideally around 30–40 min, an alternative to Logan modeling based on a 120-min acquisition is required. Such an alternative may be a bolus-infusion approach (*31*). The disadvantage of the ratio method is the need for large sample sizes and the possibility that BP_{ND} will be overestimated, especially in high-binding regions. In such study designs, the practical and financial advantages of using ^{123}I-ADAM SPECT instead of, for example, ^{11}C-labeled 3-amino-4-(2-dimethylaminomethyl-phenylsulfanyl)benzonitrile PET may vanish. In study designs permitting only small sample sizes or requiring repeated monitoring, use of ^{123}I-ADAM SPECT will require that subjects tolerate a 120-min acquisition. The Logan model with k2′ will be the most reliable quantification tool in such studies. In this setup, arterial blood sampling can be avoided. Test–retest data using this setup are necessary if such a method should be implemented.

Regional values of BP_P and BP_{ND} were consistent with the known distribution pattern of serotonin transporter in the human brain, with the highest values occurring in the thalamus, followed by the putamen, midbrain, caudatus, frontal cortex, and occipital cortex (*25*). The mean BP_P values were comparable to the mean in vitro values for specific *BP* from

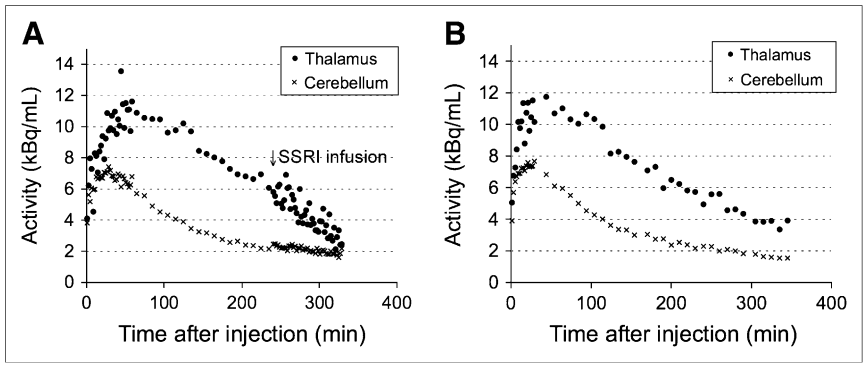

FIGURE 6. (A) Time–activity curves from subject exposed to blocking of serotonin transporter. From 240 to 270 min after injection, 0.25 mg of citalopram per kilogram of body weight was infused intravenously. From 240 min, regional binding was sampled in 2-min frames. Time–activity curve from thalamus approached cerebellar time–activity curve within the 330 min. Cerebellar binding was not displaced. (B) Time–activity curves from subject not exposed to blocking agents.

^{3}H-citalopram binding, except in the caudatus, where the binding measured by autoradiography was substantially higher (17 ± 4.2 vs. 10 ± 3.8), and in the midbrain, which in our study design was not representative of the raphe nuclei (*32*).

Delineation of a region representative of the raphe nuclei is challenging in in vivo neuroimaging because the raphe nuclei are not visible on MRI. Also, segmentation and thereby partial-volume correction cannot be performed adequately because of the poor ability to distinguish between gray and white matter in this region. Consequently, our midbrain quantification produced binding values comparable to the values in the putamen, which are lower than expected for a region comprising the superior raphe nucleus. Also, modeling of time–activity curves from the midbrain was difficult, as observed by others (*33*), probably because of the combined effects of greater noise and less reversible tracer binding in this region. In particular, the simplified reference tissue model had difficulty with this region, producing large overestimations in 2 of 7 subjects.

The specificity of ^{123}I-ADAM binding was evaluated in a blocking experiment with injection of an SSRI during acquisition. However, because of unacceptable side effects, only 2 subjects received the full blocking dose (0.25 mg of citalopram per kilogram of body weight, infused intravenously over 30 min). We might have achieved higher compliance with the blocking paradigm had we combined the blocking with an injection of ondansetron, a selective antagonist of 5-hydroxytryptamine receptor 3, with antiemetic action. As illustrated in Figure 6, the time–activity curve from the thalamus approached the cerebellar time–activity curve as an indication that blocking was achieved. The fact that cerebellar binding did not deviate from its time–activity curve supports the use of the cerebellum as a reference region, even though some specific binding is present in the cerebellum, particularly in the vermis (*25,34*).

In 2 cases, we identified a lipophilic metabolite. Although we did not identify and characterize the lipophilic metabolite, our data suggest that it does not bind specifically to serotonin transporter because the fraction did not increase after SSRI blockade, unlike the fraction of parent compound. Only 1 study, by Catafau et al., has attempted to identify metabolites of ^{123}I-ADAM in humans (*7*); in 5 subjects, lipophilic metabolites were not found in venous plasma. Catafau et al. used acetonitrile precipitation before the HPLC analysis. In baboons, no lipophilic metabolites were observed on ethyl acetate extraction or thin-layer chromatography (*30*). We cannot exclude that differences in extraction methods and HPLC analysis time might explain why other groups did not detect lipophilic metabolites. Given the lengthy retention of ^{123}I-ADAM, it is important that the HPLC measurements be run for at least 20 min to detect possible lipophilic metabolites. On the other hand, the discrepancy might reflect simply the high variability of ^{123}I-ADAM metabolism and the rarity of lipophilic metabolites. We suggest that solid-phase extraction be used in study designs requiring characterization of ^{123}I-ADAM metabolites and that whole-blood samples be kept on ice until analyzed, preferably within 30 min of sampling.

CONCLUSION

Quantification of serotonin transporter binding was more reliable by the Logan reference tissue model with $k2'$ than by the method used so far, the ratio method. The Logan model was also applicable for time–activity curves from 0 to 120 min, making the model a realistic alternative to the ratio method. Cerebellar binding was unaltered after SSRI infusion, supporting the use of the cerebellum as a reference region. Systemic metabolism of ^{123}I-ADAM is highly variable, and labeled lipophilic metabolites were present in some subjects. However, the labeled lipophilic metabolite seems not to bind specifically to serotonin transporter.

ACKNOWLEDGMENTS

We thank Karin Stahr for expert technical assistance with metabolite analyses and Gerda Thomsen and Glenna Skouboe for expert assistance with SPECT measurements. We thank Haroon Arfan, Lene Rottensten, and Inge Møller for assistance with blood sampling and Esben Hoegh Rasmussen for assistance with hardware issues. This work was supported by the Danish Medical Research Council, the Toyota Foundation, the University of Copenhagen, H:S Hovedstadens Sygehusfællesskab, and the EU 6th framework program (EC-FP6-project DiMI [LSHB-CT-2005-512146]).

REFERENCES

1. Hesse S, Barthel H, Schwarz J, Sabri O, Muller U. Advances in in vivo imaging of serotonergic neurons in neuropsychiatric disorders. *Neurosci Biobehav Rev.* 2004;28:547–563.
2. Haugbol S, Pinborg LH, Regeur L, et al. Cerebral 5-HT2A receptor binding is increased in patients with Tourette's syndrome. *Int J Neuropsychopharmacol.* 2007;10:245–252.
3. Blakely RD, De Felice LJ, Hartzell HC. Molecular physiology of norepinephrine and serotonin transporters. *J Exp Biol.* 1994;196:263–281.
4. Huang Y, Hwang DR, Narendran R, et al. Comparative evaluation in nonhuman primates of five PET radiotracers for imaging the serotonin transporters: [^{11}C]McN 5652, [^{11}C]ADAM, [^{11}C]DASB, [^{11}C]DAPA, and [^{11}C]AFM. *J Cereb Blood Flow Metab.* 2002;22:1377–1398.
5. Oya S, Choi SR, Hou C, et al. 2-((2-((dimethylamino)methyl)phenyl)thio)-5-iodophenylamine (ADAM): an improved serotonin transporter ligand. *Nucl Med Biol.* 2000;27:249–254.
6. Newberg AB, Plossl K, Mozley PD, et al. Biodistribution and imaging with ^{123}I-ADAM: a serotonin transporter imaging agent. *J Nucl Med.* 2004;45:834–841.
7. Catafau AM, Perez V, Penengo MM, et al. SPECT of serotonin transporters using ^{123}I-ADAM: optimal imaging time after bolus injection and long-term test-retest in healthy volunteers. *J Nucl Med.* 2005;46:1301–1309.
8. Catafau AM, Perez V, Plaza P, et al. Serotonin transporter occupancy induced by paroxetine in patients with major depression disorder: a ^{123}I-ADAM SPECT study. *Psychopharmacology (Berl).* 2006;189:145–153.
9. Sacher J, Asenbaum S, Klein N, et al. Binding kinetics of ^{123}I[ADAM] in healthy controls: a selective SERT radioligand. *Int J Neuropsychopharmacol.* 2007;10:211–218.
10. Booij J, de Win MM. Brain kinetics of the new selective serotonin transporter tracer [^{123}I]ADAM in healthy young adults. *Nucl Med Biol.* 2006;33:185–191.
11. Klein N, Sacher J, Geiss-Granadia T, et al. In vivo imaging of serotonin transporter occupancy by means of SPECT and [^{123}I]ADAM in healthy subjects administered different doses of escitalopram or citalopram. *Psychopharmacology (Berl).* 2006;188:263–272.

12. Klein N, Sacher J, Geiss-Granadia T, et al. Higher serotonin transporter occupancy after multiple dose administration of escitalopram compared to citalopram: an [^{123}I]ADAM SPECT study. *Psychopharmacology (Berl).* 2007;191:333–339.
13. Herold N, Uebelhack K, Franke L, et al. Imaging of serotonin transporters and its blockade by citalopram in patients with major depression using a novel SPECT ligand [^{123}I]-ADAM. *J Neural Transm.* 2006;113:659–670.
14. Uebelhack R, Franke L, Herold N, Plotkin M, Amthauer H, Felix R. Brain and platelet serotonin transporter in humans: correlation between [^{123}I]-ADAM SPECT and serotonergic measurements in platelets. *Neurosci Lett.* 2006;406: 153–158.
15. Koskela AK, Keski-Rahkonen A, Sihvola E, et al. Serotonin transporter binding of [^{123}I]ADAM in bulimic women, their healthy twin sisters, and healthy women: a SPET study. *BMC Psychiatry.* 2007;7:19.
16. Schuh-Hofer S, Richter M, Geworski L, et al. Increased serotonin transporter availability in the brainstem of migraineurs. *J Neurol.* 2007;254:789–796.
17. Erlandsson K, Sivananthan T, Lui D, et al. Measuring SSRI occupancy of SERT using the novel tracer [^{123}I]ADAM: a SPECT validation study. *Eur J Nucl Med Mol Imaging.* 2005;32:1329–1336.
18. Newberg AB, Amsterdam JD, Wintering N, et al. ^{123}I-ADAM binding to serotonin transporters in patients with major depression and healthy controls: a preliminary study. *J Nucl Med.* 2005;46:973–977.
19. Lammertsma AA, Hume SP. Simplified reference tissue model for PET receptor studies. *Neuroimage.* 1996;4:153–158.
20. Logan J. A review of graphical methods for tracer studies and strategies to reduce bias. *Nucl Med Biol.* 2003;30:833–844.
21. Woods RP, Cherry SR, Mazziotta JC. Rapid automated algorithm for aligning and reslicing PET images. *J Comput Assist Tomogr.* 1992;16:620–633.
22. Svarer C, Madsen K, Hasselbalch SG, et al. MR-based automatic delineation of volumes of interest in human brain PET images using probability maps. *Neuroimage.* 2005;24:969–979.
23. Muller-Gartner HW, Links JM, Prince JL, et al. Measurement of radiotracer concentration in brain gray matter using positron emission tomography: MRI-based correction for partial volume effects. *J Cereb Blood Flow Metab.* 1992;12: 571–583.
24. Quarantelli M, Berkouk K, Prinster A, et al. Integrated software for the analysis of brain PET/SPECT studies with partial-volume-effect correction. *J Nucl Med.* 2004;45:192–201.
25. Kish SJ, Furukawa Y, Chang LJ, et al. Regional distribution of serotonin transporter protein in postmortem human brain: is the cerebellum a SERT-free brain region? *Nucl Med Biol.* 2005;32:123–128.
26. Huang Y, Narendran R, Bae SA, et al. A PET imaging agent with fast kinetics: synthesis and in vivo evaluation of the serotonin transporter ligand [^{11}C]2-[2-dimethylaminomethylphenylthio)]-5-fluorophenylamine ([^{11}C]AFA). *Nucl Med Biol.* 2004;31:727–738.
27. Innis RB, Cunningham VJ, Delforge J, et al. Consensus nomenclature for in vivo imaging of reversibly binding radioligands. *J Cereb Blood Flow Metab.* 2007;27: 1533–1539.
28. Stahr K, Frokjaer VG, Knudsen GM. Evaluation of a metabolite assay: quantification of [^{123}I]ADAM in human plasma [abstract]. *Eur J Nucl Med Mol Imaging.* 2004;31(suppl):S485.
29. Slifstein M, Laruelle M. Effects of statistical noise on graphic analysis of PET neuroreceptor studies. *J Nucl Med.* 2000;41:2083–2088.
30. Acton PD, Choi SR, Hou C, Plossl K, Kung HF. Quantification of serotonin transporters in nonhuman primates using [^{123}I]ADAM and SPECT. *J Nucl Med.* 2001;42:1556–1562.
31. Carson RE, Channing MA, Blasberg RG, et al. Comparison of bolus and infusion methods for receptor quantitation: application to [^{18}F]cyclofoxy and positron emission tomography. *J Cereb Blood Flow Metab.* 1993;13:24–42.
32. Varnas K, Halldin C, Hall H. Autoradiographic distribution of serotonin transporters and receptor subtypes in human brain. *Hum Brain Mapp.* 2004;22:246–260.
33. Praschak-Rieder N, Wilson AA, Hussey D, et al. Effects of tryptophan depletion on the serotonin transporter in healthy humans. *Biol Psychiatry.* 2005;58:825–830.
34. Cortes R, Soriano E, Pazos A, Probst A, Palacios JM. Autoradiography of antidepressant binding sites in the human brain: localization using [^{3}H]imipramine and [^{3}H]paroxetine. *Neuroscience.* 1988;27:473–496.